Spectroscopic ellipsometry of thin film and bulk anatase (TiO_2)

G. E. Jellison, Jr.,[a] L. A. Boatner, and J. D. Budai
Oak Ridge National Laboratory, Condensed Matter Sciences Division, Oak Ridge, Tennessee 37831-6030

B.-S. Jeong and D. P. Norton
University of Florida, Department of Materials Science and Engineering, 106 Rhines Hall, Gainesville, Florida 32611

(Received 20 January 2003; accepted 18 March 2003)

Spectroscopic ellipsometry (SE) measurements were made on thin-film and single-crystal TiO_2 anatase using a two-modulator generalized ellipsometer. The TiO_2 films were epitaxially stabilized on a $LaAlO_3$ substrate in the anatase crystal structure using reactive sputter deposition. The films were highly crystalline, possessing a ''stepped surface'' morphology indicative of atomic layer-by-layer growth. The SE results for the anatase film indicate that the material is essentially oriented with the *c* axis perpendicular to the substrate, but there is some anisotropy near the interface and the surface. Corrugations of the film surface, as observed using atomic force microscopy, are consistent with a surface structure needed to create cross polarization. Accurate values of the optical functions of crystalline anatase were obtained above and below the band edge using SE. Above the band edge, both the ordinary and extraordinary complex dielectric functions exhibited two critical points. © *2003 American Institute of Physics.* [DOI: 10.1063/1.1573737]

I. INTRODUCTION

TiO_2 is an interesting wide band-gap oxide that is potentially of use in a number of applications, including transparent conducting oxides,[1] chemical sensors,[2–5] and optical components. TiO_2 occurs in three distinct polymorphs: rutile, anatase, and brookite. Anatase and rutile have different structures but possess the same crystal symmetry (tetragonal, 4/mmm, or D_{4h}). Limited work has been done on brookite (orthorhombic, mmm, or D_{2h} symmetry).[6] Anatase has an elongated unit cell (a=3.78 Å, c=9.52 Å) with two natural cleavage planes [001] and [011]. Scanning electron microscopy studies of the [001] face of naturally occurring anatase show that the surface reconstructs favoring the [011] face.[7] Undoped anatase is an insulator with a band gap reported to be ~3.2 eV[8] and a reported static dielectric constant to be[9] 31. TiO_2 can be made an *n*-type semiconductor with a carrier concentration of $\sim 10^{19}$ cm^{-3} via chemical substitution or by Ti interstitials.[10–13]

Numerous prior efforts have concentrated on the formation of anatase films that are both phase pure and highly crystalline.[9,14–24] In general, epitaxial stabilization offers a means by which anatase thin films can be obtained on lattice-matched substrates—often using processing conditions where the phase is thermodynamically unstable in the bulk. Achieving an understanding of the optical properties of epitaxial stabilized anatase thin films is necessary in order to assess the viability of these materials for a variety of photonic applications.

Since both anatase and rutile have tetragonal symmetry, they are optically anisotropic with uniaxial symmetry. That is, two refractive indices and two extinction coefficients (or, equivalently, two complex dielectric functions) are required to describe the linear interaction with light at each wavelength. The ordinary refractive index and extinction coefficients, n_o and k_o, are used to describe linear light interactions for light polarized perpendicular to the *c* axis of the crystal, while the extraordinary refractive index and extinction coefficient, n_e and k_e, are used for light polarized along the *c* axis. As can be seen from the optical functions of rutile presented in Refs. 25–27, the rutile form of TiO_2 is highly anisotropic, both above and below the band gap. Below the band gap, rutile has a very large birefringence[25] $\Delta n=(n_e-n_o)\sim 0.27$, making rutile a very useful optical material.

Similarly, one expects that the optical functions of anatase will also be significantly anisotropic, but quite different from those of rutile. Other than the work of Ref. 24, very little work of this kind exists in the literature. It is the purpose of this article to discuss the spectroscopic ellipsometric measurements of both thin-film and bulk anatase, performed using the two-modulator generalized ellipsometer (2-MGE).[28] This instrument, briefly described below, is capable of measuring the normal ellipsometric parameters, as well as the cross-polarization parameters from an optical reflection experiment, thereby allowing for the complete determination of the optical functions of a suitably oriented anisotropic material from a single measurement.

II. EXPERIMENT

A. Sample preparation

The thin-film sample of anatase was fabricated on a $LaAlO_3$ substrate in a reactive rf magnetron sputter deposition system equipped with a load-lock for substrate exchange. A quartz lamp heater provided for substrate heating up to 750 °C. Ti sputtering targets of 2 in. diameter were used. The target-to-substrate distance was approximately 15 cm. The base pressure of the deposition system was on the

[a]Electronic mail: jellisongejr@ornl.gov

 © 2003 American Institute of Physics

Downloaded 11 Sep 2009 to 160.91.157.167. Redistribution subject to AIP license or copyright; see http://jap.aip.org/jap/copyright.jsp

order of 5×10^{-8} Torr. For epitaxially stabilized anatase film growth, (001) $LaAlO_3$ was chosen as the substrate as it provides a lattice mismatch on the order of 0.2%. The substrates were cleaned in trichloroethylene, acetone, and ethanol prior to mounting on the sample platen with Ag paint. Oxygen was provided through a mass-flow control valve.

The crystalline sample of anatase was naturally occurring, and the sample surface was obtained by using the natural cleavage plane along a [011] face. For this orientation, the optic axis makes an angle of 68.3° with respect to the sample surface normal. The sample surface was cleaned with a methanol rinse and N_2 drying before the measurement.

B. Ellipsometric measurement

The optical functions of thin-film and bulk anatase were determined using the two-modulator generalized ellipsometer (2-MGE).[28] Light reflection from a nondepolarizing sample can be conveniently expressed in terms of its Jones matrix, which is given by[29]

$$\mathbf{J}=\begin{pmatrix} r_{pp} & r_{ps} \\ r_{sp} & r_{ss} \end{pmatrix}=r_{ss}\begin{pmatrix} \rho_{pp} & \rho_{ps} \\ \rho_{sp} & 1 \end{pmatrix}, \tag{1}$$

where each of the elements of **J** are complex. Therefore, six elements are required to completely specify the normalized matrix **J**. The complex cross-polarization terms ρ_{sp} and ρ_{ps} are normally zero for isotropic samples, but can be nonzero for anisotropic samples. This is because the *s*- and *p*-polarization states are no longer eigenmodes for reflection from anisotropic samples. The 2-MGE is capable of measuring the six elements of the complex ρ_{pp}, ρ_{sp}, and ρ_{ps} simultaneously. If the sample is appropriately aligned (that is, if ρ_{sp} and ρ_{ps} are significantly different from 0), then only a single measurement is required to determine all of the optical functions (n_o, k_o, n_e, k_e).

The details of the 2-MGE are discussed in Ref. 28. The instrument consists of two polarizer-photoelastic modulator pairs, one acting as the polarization-state generator (PSG), the other as the polarization-state analyzer (PSA). The modulators are operated at different frequencies ($\omega_0=50.2$ and $\omega_1=60.2$ kHz), so the resulting intensity wave form at the detector is of the form

$$I(t)=I_{dc}+I_{XO}X_O+I_{YO}Y_O+I_{X1}X_1+I_{Y1}Y_1+I_{X0X1}X_0X_1 + I_{X0Y1}X_0Y_1+I_{Y0X1}Y_0X_1+I_{Y0Y1}Y_0Y_1, \tag{2}$$

where

$$X_i=\sin[A_i\ \sin(\omega_i t)], \tag{3a}$$

$$Y_i=\cos[A_i\ \sin(\omega_i t)], \quad i=0,1. \tag{3b}$$

The Bessel angles A_i are proportional to the modulating amplitude of each modulator. Using Fourier analysis, the eight coefficients $I_{X0}, I_{Y0}, I_{X1}, I_{Y1}, I_{X0X1}, I_{X0Y1}, I_{Y0X1}$, and I_{Y0Y1} are measured relative to I_{dc} which serves as a normalization factor. If the instrument is properly calibrated and aligned,[28] the eight parameters are independent and are equal to eight different elements of the normalized Mueller matrix (possibly times a sign factor) associated with light reflection from the sample surface. For azimuthal orientations of the PSG and the PSA that are (0°,±45°), (90°,±45°),(±45°,0°), or (±45°,90°), then either the upper-right or the lower-left block of the sample Mueller matrix is completely measured. If the sample is nondepolarizing then light reflecting from the sample can be described using the sample Mueller–Jones matrix and all six elements of the normalized Jones matrix **J** can be determined (see Refs. 28 and 29 for details).

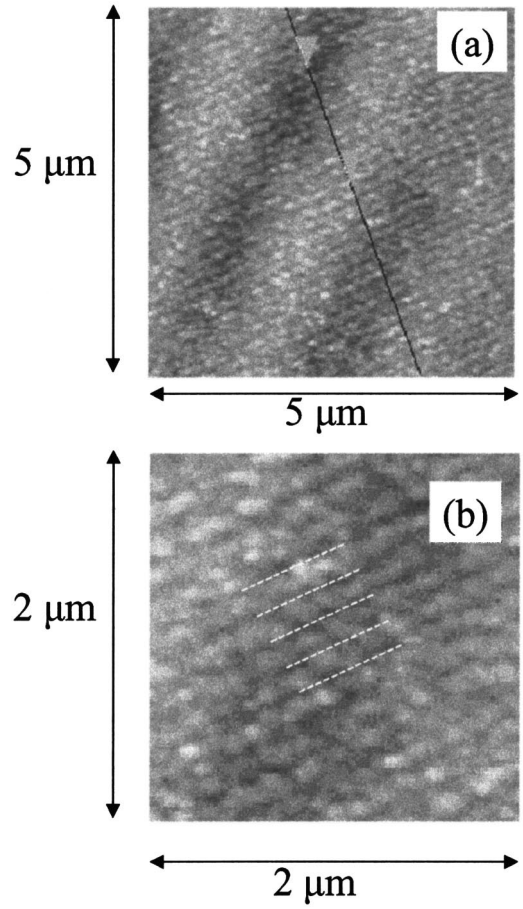

FIG. 1. Atomic force microscope (a) low resolution and (b) high resolution scan of anatase film grown at $P(O_2)=10^{-3}$ Torr and 750 °C, showing the stepped growth surface with a terrace spacing of ~160 nm.

III. RESULTS AND DISCUSSION

In terms of crystallinity and surface morphology, the anatase films grown using O_2 were excellent. Films deposited at 700 °C and $P(O_2)=10^{-3}$ Torr were phase-pure anatase with no evidence of rutile as a secondary phase. The epitaxial relationship between the film and substrate, as determined by four-circle x-ray diffraction, is $(001)[110]_{LaAlO_3}//(001)[110]_{anatase}$, as reported elsewhere.[30,31] The surface morphology exhibits evidence for step-flow or atomic layer-by-layer growth in atomic force microscopy (AFM) images. Figure 1 is an AFM image showing the growth morphology defined by surface terraces. The rms roughness for this film is 2.1 nm.

Figure 2 shows the complex reflection ratios measured using the 2-MGE from the anatase/$LaAlO_3$ sample (with the *c* axis of the anatase perpendicular to the substrate) as a function of photon energy with an angle of incidence of 65°.

Downloaded 11 Sep 2009 to 160.91.157.167. Redistribution subject to AIP license or copyright; see http://jap.aip.org/jap/copyright.jsp

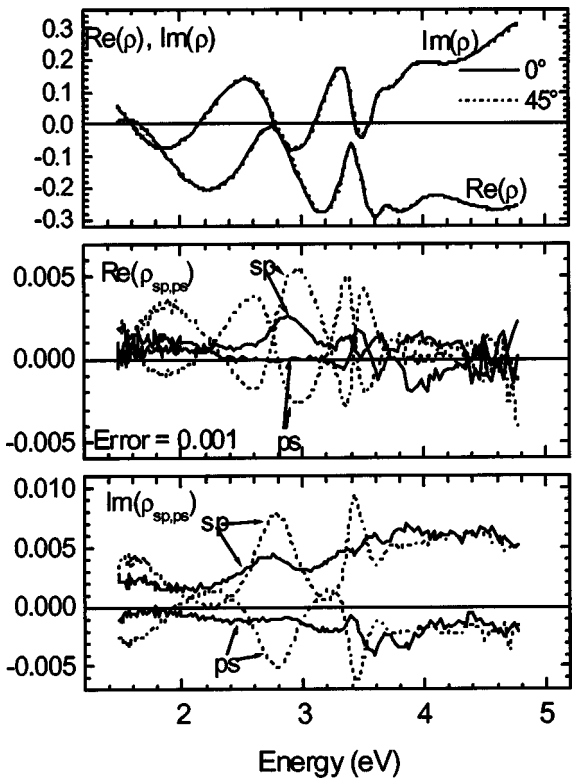

FIG. 2. Real and imaginary parts of the complex reflection ratios from an ellipsometry experiment at an angle of incidence of 65°. The solid lines refer to the experiment where the (001) axis of the substrate was aligned with the plane of incidence, while the dotted lines refer to the case where this angle is 45°.

Three sets of measurements were taken at different angles γ of the substrate (001) axis with respect to the plane of incidence (the 90° measurement is not shown). There is very little variation of the standard ellipsometric reflection ratio ρ with γ. However, interference oscillations are easily observable in the ρ_{sp} and ρ_{ps} reflection ratios when $\gamma=\pm 45°$, which is not observed with the measurements taken at $\gamma=0°$ (or at $\gamma=90°$, not shown). Well above the band edge (~3.8 eV), no interference oscillations are observed, bu the imaginary part of ρ_{sp} is ~0.006.

Ideally, one would expect no cross polarization from a *c*-axis-perpendicular film on a cubic substrate. However, the displaced $\mathrm{Im}(\rho_{sp})$ and the oscillations observed when $\gamma=45°$ indicate that the sample is not a simple *c*-axis perpendicular film on a cubic substrate. The displaced $\mathrm{Im}(\rho_{sp})$ above the band edge indicates that either the *c* axis of the film is off normal by a small amount and randomly oriented, or that the surface roughness is creating some cross polarization. The oscillations observed below ~3.4 eV for the $\gamma=45°$-oriented sample (but not for the $\gamma=0°$-oriented sample) indicate that there is a significant interfacial region between the substrate and the film where the *c* axis is not normal to the substrate.

In order to analyze the data shown in Fig. 2, it is necessary to model the near-surface region of the film.[28] For the determination of the film thicknesses, the photon energies were restricted to the transparent region (~1.48–3.1 eV), and the near-surface region was modeled using a five-medium structure: air/surface roughness/anatase film/interfacial layer/$LaAlO_3$. The surface roughness was modeled using the Bruggeman effective medium approximation[32] using 50% anatase and 50% voids. In this photon energy region (below the band edge), the anatase film was modeled using a simple Sellmeier approximation:

$$n(\lambda)^2=1+\frac{A\lambda^2}{\lambda^2-\lambda_0^2}, \tag{4}$$

where λ_0 and A are fitted parameters and λ is the wavelength of light. The interfacial layer was modeled using the Sellmeier approximation, with a different value of A, but with the value of λ_0 set to 255 nm. (This is close to the final value of λ_0 for the film, and was fixed to reduce the number of fitted parameters.) The $LaAlO_3$ substrate was also described using Eq. (4), where $\lambda_{0\mathrm{sub}}$ was set to 126 nm (from independent measurements), and A was treated as a fitted parameter. All told, there were seven fitting parameters, and the results of this fit are summarized in Table I.

TABLE I. The results of the fitting procedure of the data shown in Fig. 1 using a five-medium model (including air as the ambient), resulting in a final $\chi^2=0.28$. Fitted parameters include a 2σ error estimation, while set parameters have no associated error. The photon energy span was restricted to 1.48–3.10 eV for this fit.

Layer	Thickness (nm)	Sellmeier A	Sellmeier λ_o (nm)
Surface roughness	4.1±0.1		
Anatase film	159±1	4.73±0.03	233±2
Interface	19±2	3.82±0.1	255
$LaAlO_3$ substrate		3.19±0.02	126

Using the parameters shown in Table I, it is possible to obtain approximate values of the refractive index $\langle n\rangle$ and the extinction coefficient $\langle k\rangle$ of the anatase film from the 0° data in some regions of the spectrum (see Fig. 3). (Here, the notation $\langle n\rangle$ and $\langle k\rangle$ indicates that the calculated values of n and k contain contributions from both the ordinary and extraordinary values; this is obviously different from the normal ellipsometric definitions of the pseudo refractive index and pseudo extinction coefficient.) The values of $\langle n\rangle$ below the band edge are just the calculated n from the Sellmeier approximation, while the values of $\langle n\rangle$ and $\langle k\rangle$ above the band edge are calculated from the ellipsometric data—correcting for the surface roughness thickness shown in Table I. Aspnes[33] has shown that if the magnitude of the complex dielectric function is much greater than 1, then ellipsometric measurements of a *c*-axis perpendicular sample will be most sensitive to the ordinary refractive index and extinction coefficient n_o and k_o, so $\langle n\rangle$ and $\langle k\rangle$ should be reasonably close to n_o and k_o for anatase.

For comparison purposes, spectroscopic ellipsometry measurements were also made using a naturally occurring sample of anatase, where the reflection face is the [011] natural cleavage plane. Using the ellipsometric data well below the band edge, it is possible to estimate the surface roughness, assuming that it can be modeled using the Bruggeman effective medium approximation according to the procedure described in Refs. 25 and 29. Once the surface roughness is known, the ellipsometric data can be used to determine the

Downloaded 11 Sep 2009 to 160.91.157.167. Redistribution subject to AIP license or copyright; see http://jap.aip.org/jap/copyright.jsp

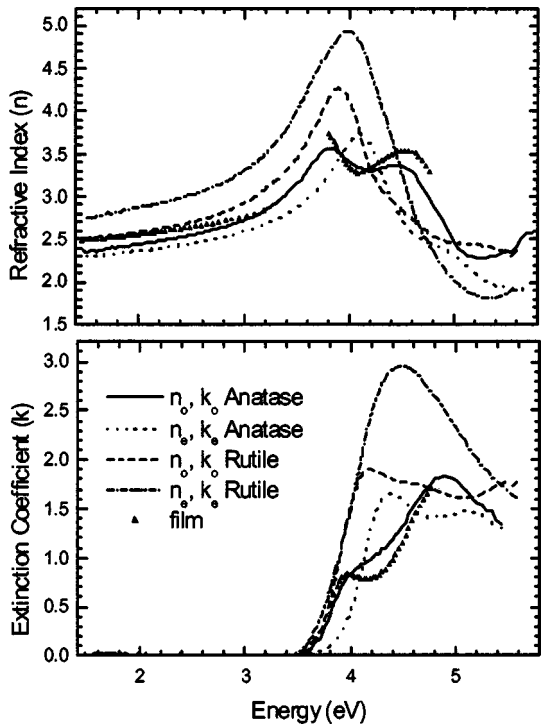

FIG. 3. The refractive index and extinction coefficient bulk anatase, rutile, and thin-film anatase determined from the spectroscopic ellipsometry data.

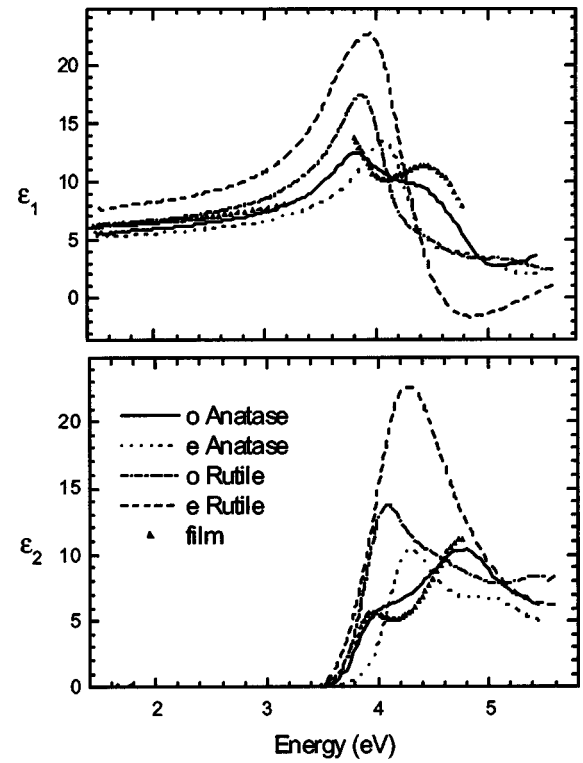

FIG. 4. The complex dielectric function for bulk anatase, rutile, and thin-film anatase, determined from the values shown in Fig. 3.

complex refractive indices (n_o, k_o, n_e, and k_e, where the o index indicates the ordinary values and the e index indicates the extraordinary values). These values are shown in Fig. 3. It is also possible to display the complex refractive index in terms of the complex dielectric function ($\varepsilon_1 = n^2 - k^2$; $\varepsilon_2 = 2nk$) and the optical absorption coefficient ($\alpha = 4\pi k/\lambda$), as shown in Figs. 4 and 5. These figures also show comparison values of the complex indices of refraction of rutile, determined down to 222 nm in a similar fashion to the values shown in Ref. 25.

Clearly, the complex refractive indices of anatase and rutile are quite different. Below the band edge, rutile has a higher refractive index, as well as a greater value of birefringence, than does anatase. Above the band edge, two critical points (that is, features in the ε_2 spectra) are observable in the spectra of anatase (a shoulder at 3.8 eV and a broad peak at 4.8 eV for ε_{2o} and a peak at 4.3 and a shoulder at 5.05 eV for ε_{2e}), while rutile exhibits one peak (at 4.1 eV for ε_{2o} and a much stronger one at 4.3 eV for ε_{2e}). The absorption coefficients for rutile (both α_o and α_e) and α_o for anatase fall off rapidly with decreasing photon energy near the band edge. However, the α_e for anatase falls off much more gradually.

The values of ε_2 can be compared with the results of the band structure calculations of Mo and Ching.[34] The values of ε_{2o} and ε_{2e} (denoted as ε_{2xy} and ε_{2z}, respectively, in Ref. 34) are shown in Fig. 6 for rutile and anatase. As can be seen, other than ε_{2e} for rutile, the magnitudes of the peaks generally agree. However, there are significant differences between the values of ε_2 determined experimentally and from the calculations. In all cases, the calculations indicate significant optical absorption above ~2.5–3 eV, which is not observed experimentally. Furthermore, the two peaks in ε_2 observed in both the o and e spectra of anatase are not well represented in the calculated spectra.

The spectroscopic ellipsometry results for the thin film show that it is somewhat different than either rutile or anatase. The effective spectroscopic refractive index of the anatase film $\langle n \rangle$ is somewhat lower than that of either n_o and n_e of rutile, but higher than either n of anatase. However, the values of k above the band edge resemble the values of k_o of anatase, which is to be expected from the approximation of Aspnes.[33]

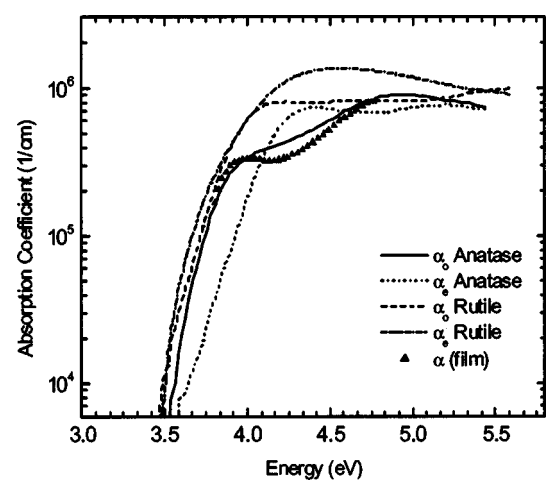

FIG. 5. The optical absorption coefficient for bulk anatase, rutile, and thin-film anatase, determined from the values shown in Fig. 3.

Downloaded 11 Sep 2009 to 160.91.157.167. Redistribution subject to AIP license or copyright; see http://jap.aip.org/jap/copyright.jsp

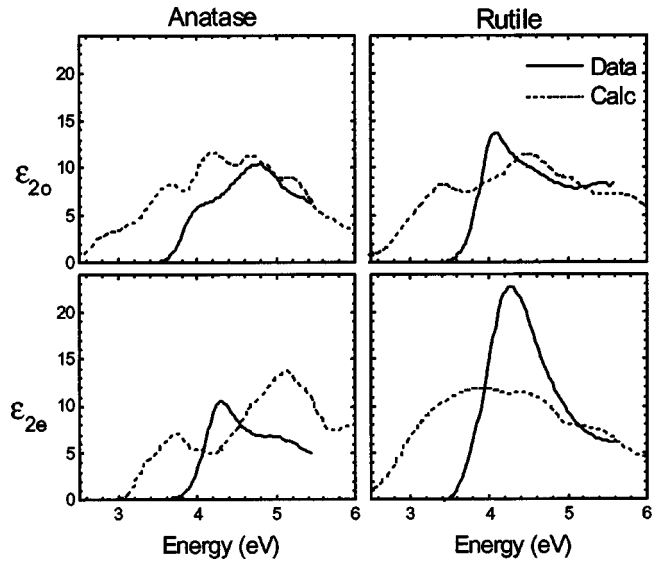

FIG. 6. The imaginary part of the complex dielectric function for both rutile and anatase, compared with the band structure calculations of Mo and Ching.

Generally, accurate spectroscopic ellipsometry measurements of the absorption coefficient α can only be made for values of $\alpha > \sim 10^4$ cm^{-1}, and optical transmission measurements can be used to measure α for $\alpha < \sim 100$ cm^{-1}. As a result there is a range of absorption coefficients from $\sim 10^2$ to 10^4 cm^{-1} where it is very difficult to obtain good measurements of the absorption coefficient. In addition, optical absorption in this region is often complicated by surface scattering, Urbach tail absorption, and other nonintrinsic effects that can contribute to the measured optical absorption. As a result, only estimates of the optical and edge can often be made from either ellipsometry or transmission measurements.[35–37] If we define the optical band edge as the photon energy where the value of $\alpha = 10^4$ cm^{-1}, then the band edges are E_{go}(rutile)$=3.84$eV, E_{ge}(rutile$=3.51$, E_{go}(anatase)$=3.57$ eV, and E_{ge}(anatase)$=3.67$. These values are considerably higher than those obtained from transmission measurements.[35–37]

ACKNOWLEDGMENTS

This work was partially supported by the Army Research Office through research Grant No. DAAD 19-01-1-0508, and by the U.S. Department of Energy under Contract No. DE-AC-00OR22725 with the Oak Ridge National Laboratory, managed by UT-Battelle, LLC. The authors would also like to acknowledge the staff of the Major Analytical Instrumentation Center, Department of Materials Science and Engineering, University of Florida, for their assistance with this work.

[1] H. L. Hartnagel, A. L. Dawar, A. K. Jain, and C. Jagadish, *Semiconducting Transparent Thin Films* (Institute of Physics, Bristol, 1995).
[2] H. Meixner and U. Lampe, Sens. Actuators B **33**, 198 (1996).
[3] A. Rothschild, F. Edelman, Y. Komem, and F. Cosandey, Sens. Actuators B **67**, 282 (2000).
[4] N. Savage, B. Chwieroth, A. Ginwalla, B. R. Patton, S. A. Akbar, and P. K. Dutta, Sens. Actuators B **79**, 17 (2001).
[5] L. Chow, M. Yuen, P. Chan, and A. Cheung, Sens. Actuators B **76**, 310 (2001).
[6] M. Koesch, S. Cassaignon, I. Suillemoles, and J. R. Jolivet, Thin Solid Films **403-404**, 312 (2002).
[7] N. Ruzycki, G. S. Herman, L. A. Boatner, and U. Diebold, Surf. Sci. Lett. **529**, L239 (2003).
[8] H. Tang, H. Berger, P. E. Schmid, and F. Levy, Solid State Commun. **92**, 267 (1994).
[9] H. Tang, K. Prasad, R. Sanjines, P. E. Schmid, and F. Levy, J. Appl. Phys. **75**, 2042 (1994).
[10] E. Yagi, R. R. Hasiguti, and M. Aono, Phys. Rev. B **54**, 7945 (1996).
[11] J. W. DeFord and O. W. Johnson, J. Appl. Phys. **54**, 889 (1983).
[12] L. Forro, O. Chauvet, D. Emin, L. Luppiroli, H. Berger, and F. Lévy, J. Appl. Phys. **75**, 633 (1994).
[13] A. Bernasik, M. Radecka, M. Rekas, and M. Sloma, Appl. Surf. Sci. **66**, 240 (1993).
[14] C. K. Ong and S. J. Wang, Appl. Surf. Sci. **185**, 47 (2001).
[15] G. S. Herman and Y. Gao, Thin Solid Films **397**, 157 (2001).
[16] S. Yamamoto, T. Sumita, Sugiharuto, A. Miyashita, and H. Naramoto, Thin Solid Films **401**, 88 (2001).
[17] M. Schvisky, K. Kukli, J. Aarik, J. Lu, and A. Harsta, J. Cryst. Growth **235**, 293 (2002).
[18] T. Miyagi, T. Ogawa, M. Kamei, Y. Wada, T. Yamazaki, E. Ohta, and T. Sato, Jpn. J. Appl. Phys., Part 2 **40**, L404 (2001).
[19] P. A. Morris Hotsenpiller, G. A. Wilson, A. Roshko, J. B. Rothman, and G. S. Rohrer, J. Cryst. Growth **166**, 779 (1996).
[20] M. Murakami, Y. Matsumoto, K. Nakajima, T. Makino, Y. Segawa, T. Chikyow, P. Ahmet, M. Kawasaki, and H. Koinuma, Appl. Phys. Lett. **78**, 2664 (2001).
[21] Sugiharto, S. Yamamoto, T. Sumita, and A. Miyashita, J. Phys.: Condens. Matter **13**, 2875 (2001).
[22] S. Chen, M. G. Mason, H. J. Gysling, G. R. Paz-Pujalt, T. N. Blanton, T. Castro, K. M. Chen, C. P. Fictorie, W. L. Gladfelter, A. Franciosi, P. I. Cohen, and J. F. Evans, J. Vac. Sci. Technol. A **11**, 2419 (1993).
[23] W. Sugimura, A. Yamazaki, H. Shigetani, J. Tanaka, and T. Mitsuhashi, Jpn. J. Appl. Phys., Part 1 **36**, 7358 (1997).
[24] T. M. R. Viseu, B. Almeida, M. Stchakovsky, B. Drevillon, M. I. C. Ferreira, and J. B. Sousa, Thin Solid Films **401**, 216 (2001).
[25] G. E. Jellison, Jr., F. A. Modine, and L. A. Boatner, Opt. Lett. **22**, 1808 (1997).
[26] M. Schubert, B. Rheinlander, J. A. Woollam, B. Johs, and C. M. Herzinger, J. Opt. Soc. Am. A **13**, 875 (1996).
[27] T. Tiwald and M. Schubert, Proc. SPIE **4103**, 19 (2000).
[28] G. E. Jellison, Jr. and F. A. Modine, Appl. Opt. **36**, 8184 (1997); **36**, 8190 (1997).
[29] G. E. Jellison, Jr., Thin Solid Films **313-314**, 33 (1998).
[30] B.-S. Jeong, J. D. Budai, and D. P. Norton, Thin Solid Films **422**, 166 (2002).
[31] J. Y. Huang, B. H. Park, D. Jan, X. Q. Pan, Y. T. Zhu, and Q. X. Jia, Philos. Mag. A **82**, 735 (2002).
[32] D. A. G. Bruggeman, Ann. Phys. (Leipzig) **24**, 636 (1935).
[33] D. E. Aspnes, J. Opt. Soc. Am. **70**, 1275 (1980).
[34] S.-D. Mo and W. Y. Ching, Phys. Rev. B **51**, 13023 (1995).
[35] H. Tang, F. Levy, H. Berger, and P. E. Schmid, Phys. Rev. B **52**, 7771 (1995).
[36] A. Aoki and G. Nogami, J. Electrochem. Soc. **143**, L191 (1996).
[37] G. K. Boschloo, A. Goossens, and J. Schoonman, J. Electro-chem. Soc. **144**, 1311 (1997).

Downloaded 11 Sep 2009 to 160.91.157.167. Redistribution subject to AIP license or copyright; see http://jap.aip.org/jap/copyright.jsp